Solid State Communications 343 (2022) 114663

Contents lists available at ScienceDirect

Solid State Communications

journal homepage: www.elsevier.com/locate/ssc

Effect of lithium substitution with sodium on electrical properties in $La_{0.5}Li_{0.5-x}Na_xTiO_3$ and $La_{0.67}Li_{0.2-y}Na_yTi_{0.8}Al_{0.2}O_3$ solid solutions

Tatiana Plutenko [a], Oleg V'yunov [a,*], Oleg Yanchevskii [a], Oleksandr Fedorchuk [a], Anatolii Belous [a], Maxym Plutenko [b]

[a] V. I. Vernadsky Institute of General and Inorganic Chemistry, Department of Solid State Chemistry, 32/34 acad. Palladina ave. Kyiv, 03142, Ukraine
[b] Taras Shevchenko National University of Kyiv, Department of Physical Chemistry, Volodymyrska street, 64/13, Kyiv, 01601, Ukraine

ARTICLE INFO

Communicated by F. Peeters

ABSTRACT

Li-containing $La_{0.5}Li_{0.5-x}Na_xTiO_3$ and $La_{0.67}Li_{0.2-y}Na_yTi_{0.8}Al_{0.2}O_3$ solid solutions have been obtained by solid-state reaction route that involves chemical decomposition reactions. Complex impedance spectroscopy measurements demonstrate that the electrical properties in $La_{0.5}Li_{0.5-x}Na_xTiO_3$ and $La_{0.67}Li_{0.2-y}Na_yTi_{0.8}Al_{0.2}O_3$ systems depend on different areas of the ceramic's grain and can be represented by the equivalent circuit consisting of two (when $x = 0.5$, $y = 0.2$) and three series-connected elements ($0 \leq x \leq 0.4$, $0 \leq y \leq 0.15$). It has been shown that an increase in sodium concentration leads to a decrease in the ceramic's grain size for $La_{0.5}Li_{0.5-x}Na_xTiO_3$ and $La_{0.67}Li_{0.2-y}Na_yTi_{0.8}Al_{0.2}O_3$ solid solutions. Substitution of lithium ions by sodium leads to an increase in the unit cell volume of the perovskite structure. It has been demonstrated that $La_{0.67}Li_{0.14}Na_{0.06}Ti_{0.8}Al_{0.2}O_3$ and $La_{0.5}Li_{0.4}Na_{0.1}TiO_3$ materials with low sodium concentration have the maximum value of dielectric constant.

1. Introduction

Solid-state Li-ion conducting perovskites are currently attracting considerable research attention as they present a viable opportunity for applications when compared to conventional liquid electrolyte-based devices [1–10]. Lithium lanthanum titanate is one of the most promising solid electrolytes has been found to show high ionic conductivity of 10^{-3} S cm^{-1} at room temperature [11].

The conductivity of lithium ions depends on the ion distribution and the presence of vacancies in the lanthanum sublattice [12–14]. The movement of lithium ions occurs along the structural conduction channels formed by oxygen ions and is limited by the presence of "bottlenecks" in the conduction channels [15]. When lanthanum ions are replaced by ions with a large ionic radius, the "bottleneck" size increases, while the number of vacancies in the A sublattice of the structural type ABO_3 perovskite decreases [16–19]. When lithium ions are partially replaced by sodium ions, sodium ions occupy the center of position A, while lithium is located at the center of the square plane face formed by oxygen [16,17].

High dielectric, low loss perovskite materials [20–23] are attracting considerable attention and can store more energy than low dielectric materials [24–37]. It was shown that a high dielectric constant ($\varepsilon \geq 1000$) was observed in the $La_{0.67}Li_xTi_{1-x}Al_xO_3$ ($0.15 \leq x \leq 0.3$) system. The origin of high dielectric constant value can be explained by barrier layer capacitor associated with grain boundary effects [38]. It has been found that in $La_{0.67}Li_xTi_{1-x}Al_xO_3$ system $La_{0.67}Li_{0.2}Ti_{0.8}Al_{0.2}O_3$ solid solution has the maximum dielectric constant in a wide frequency range [39].

In this work, the effect of lithium substitution for sodium in high dielectric constant $La_{0.5}Li_{0.5-x}Na_xTiO_3$ and $La_{0.67}Li_{0.2-y}Na_yTi_{0.8}Al_{0.2}O_3$ materials has been studied. The parameters of the unit cell and the ceramic's grain sizes of $La_{0.5}Li_{0.5-x}Na_xTiO_3$ and $La_{0.67}Li_{0.2-y}Na_yTi_{0.8}Al_{0.2}O_3$ solid solutions were determined. Using complex impedance the effect of sodium concentration on the equivalent circuit parameters and the dielectric characteristics (ϵ and tg δ) of materials was established.

2. Material and methods

Samples were obtained from stoichiometric amounts of dried Li_2CO_3 (Merck), Na_2CO_3 (Merck), La_2O_3 (Aldrich 99.99%), Al_2O_3 (Aldrich

* Corresponding author.
E-mail addresses: taplutenko@gmail.com (T. Plutenko), vyunov@ionc.kiev.ua (O. V'yunov), yancholz@gmail.com (O. Yanchevskii), alex1377c9@gmail.com (O. Fedorchuk), belous@ionc.kiev.ua (A. Belous), plutenkom@gmail.com (M. Plutenko).

https://doi.org/10.1016/j.ssc.2022.114663
Received 21 May 2020; Received in revised form 21 October 2021; Accepted 12 January 2022
Available online 13 January 2022

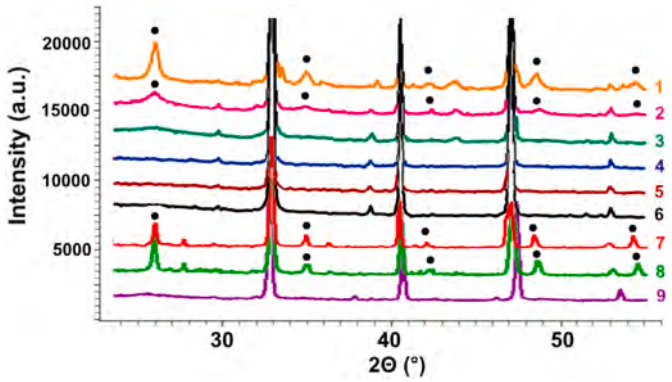

Fig. 1. XRPD of $La_{0.5}Li_{0.5-x}Na_xTiO_3$ at x = 0 (1), 0.1 (2), 0.2 (3), 0.3 (4), 0.4 (5), 0.5 (6) and $La_{0.67}Li_{0.2-y}Na_yTi_{0.8}Al_{0.2}O_3$ at y = 0 (7), 0.06 (8), 0.15 (9). (symbols "•" denotes the phase with tetragonal space group P4/mmm).

Table 1
Unit cell volume of $La_{0.5}Li_{0.5-x}Na_xTiO_3$ ($0 \leq x \leq 0.5$) and $La_{0.67}Li_{0.2-y}Na_yTi_{0.8}Al_{0.2}O_3$ ($0 \leq y \leq 0.2$) samples with R-3c space group.

$La_{0.5}Li_{0.5-x}Na_xTiO_3$ system						
X	0	0.1	0.2	0.3	0.4	0.5
V, Å^3	347.4(2)	347.6(2)	347.7(2)	347.9(2)	348.1(2)	348.6(9)
$La_{0.67}Li_{0.2-y}Na_yTi_{0.8}Al_{0.2}O_3$ system						
Y	0	0.04	0.06	0.10	0.15	0.2
V, Å^3	345.86(4)	346.1(3)	346.3(3)	346.66(2)	346.8(5)	347.4(4)

99.99%), and TiO_2 (Aldrich 99%) by solid-state reaction technique. Li_2CO_3 and Na_2CO_3 compounds were dried at 300 °C, La_2O_3 at 800 °C, and TiO_2 at 600 °C. The mixtures $La_{0.5}Li_{0.5-x}Na_xTiO_3$ and $La_{0.67}Li_{0.2-y}Na_yTi_{0.8}Al_{0.2}O_3$ were ground in an agate mortar with acetone and calcined in air for 4 h at 1100 °C and 1200 °C, respectively. The rate of temperature increase was 200 °C/hour. The phases were characterized by X-ray powder diffractometry (XRPD) using DRON-4-07 diffractometer (Cu *K*α radiation; 40 kV, 20 mA). The calcined powders were ground and pressed into pellets under a pressure of 500 kg/cm^2 (50 MPa). The pellets were sintered at 1300-1330 °C depending on Na content (6 h). Finally, samples with 2 mm thickness were cut out from prepared raw ceramic.

Grain sizes of ceramic samples of $La_{0.5}Li_{0.5-x}Na_xTiO_3$ and $La_{0.67}Li_{0.2-y}Na_yTi_{0.8}Al_{0.2}O_3$ systems were determined using a scanning electron microscope JEM 10CX II (JEOL) and scanning electron microscope SEC miniSEM SNE 4500 MB equipped with EDAX Element PV6500/00 F spectrometer. Sintered cylindrical pellets 10 mm in diameter and 2 mm thick, with evaporated electrodes, were used for electrical measurements.

Impedance spectroscopy measurements were conducted using a 1260 Impedance/Gain phase Analyzer (Solartron Analytical). The model of the equivalent circuit and the value of its components were determined using the ZView® software (Scribner Associates Inc., USA).

3. Results and discussion

X-ray diffraction patterns of $La_{0.67}Li_{0.2-y}Na_yTi_{0.8}Al_{0.2}O_3$ ($0 \leq y \leq 0.2$) and $La_{0.5}Li_{0.5-x}Na_xTiO_3$ ($0 \leq x \leq 0.5$) ceramic samples for 12 h in planetary ball mill (Fig. 1) showed that solid solutions have rhombohedral (trigonal) symmetry (space group R-3c, N° 167). It was found that with an increase in sodium concentration, the volume of the unit cell increases, which is associated with the difference in the ionic radii of sodium and lithium (Table 1).

For $0 \leq y \leq 0.06$, $0 \leq x \leq 0.1$, in XRPD spectra additional lines of phases $La_{0.5}Li_{0.5-x}Na_xTiO_3$ and $La_{0.67}Li_{0.2-y}Na_yTi_{0.8}Al_{0.2}O_3$ with tetragonal symmetry (space group P4/mmm, N° 123) in the XRPD spectra are observed (Fig. 1). Tetragonal and rhombohedral phases are identical in chemical composition. There is nanoscale ordering in the domains of the tetragonal phase, while in the rhombohedral phase, there is no ordering of domains. With an increase in sodium concentration, the tetragonal phase disappears [40,41].

The XRPD results showed that $La_{0.5}Li_{0.5-x}Na_xTiO_3$ ($0 \leq x \leq 0.5$) solid solutions are formed at temperatures higher than 1100 °C whereas $La_{0.67}Li_{0.2-y}Na_yTi_{0.8}Al_{0.2}O_3$ ($0 \leq y \leq 0.2$) solid solutions are formed at temperatures higher than 1200 °C. Solid-state reaction technique involves chemical decomposition reactions of carbonates Li_2CO_3 and Na_2CO_3. The reaction in a mixture of solid reactants starts at the points of contact between the initial components and continues successively by ionic interdiffusion at high temperatures.

It has been shown that single-phase $La_{0.5}Li_{0.5-x}Na_xTiO_3$ solid solutions are formed at temperatures above 1100 °C. Intermediate phases in Na-doped ceramics are $La(OH)_3$, $La_2O_2CO_3$, Na_4TiO_4, $Na_4Ti_5O_{12}$, $Na_2Ti_2O_5$, Li_2TiO_3, $Li_2Ti_2O_5$, $Li_2Ti_3O_7$, $La_2Ti_2O_7$, $La_{0.5}Li_{0.5}TiO_3$ and $La_{0.5}Na_{0.5}TiO_3$. Final solid solution $La_{0.5}Li_{0.5-x}Na_xTiO_3$ is formed by the interaction:

$$x La_{0.5}Na_{0.5}TiO_3 + (1-x) La_{0.5}Li_{0.5}TiO_3 \xrightarrow{1100^\circ C} La_{0.5}Li_{0.5-x}Na_xTiO_3$$

In $La_{0.67}Li_{0.2-y}Na_yTi_{0.8}Al_{0.2}O_3$ ($0 \leq y \leq 0.2$) solid solutions, the intermediate phases are $La(OH)_3$, $La_2O_2CO_3$, Li_2TiO_3, $Li_2Ti_2O_5$, $Li_2Ti_3O_7$, Na_2TiO_3, $Na_2Ti_2O_5$, $La_2Ti_2O_7$, $La_{2/3}TiO_3$, $LaAlO_3$, $La_{0.67}Li_{0.2}Ti_{0.8}Al_{0.2}O_3$,

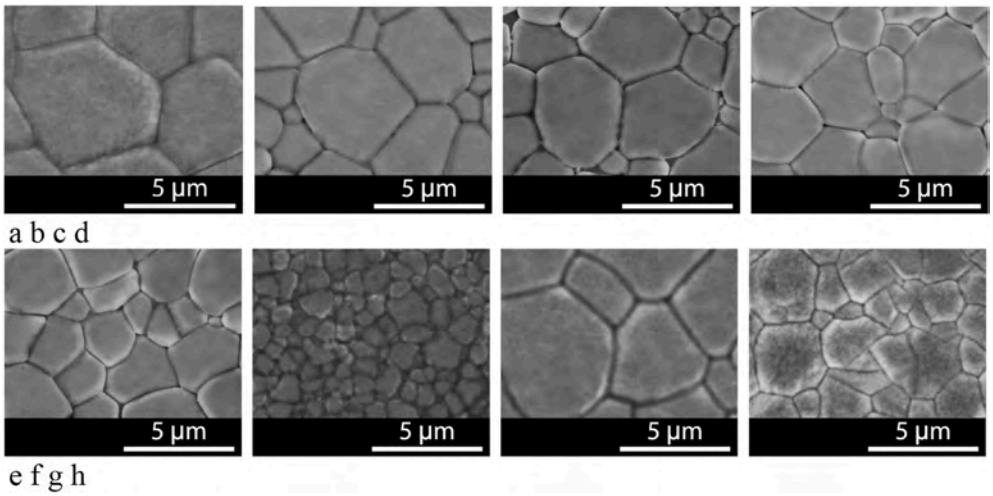

Fig. 2. Micrographs of $La_{0.5}Li_{0.5-x}Na_xTiO_3$ and $La_{0.67}Li_{0.2-y}Na_yTi_{0.8}Al_{0.2}O_3$ at $x = 0$ (a), 0.1 (b), 0.2 (c), 0.3 (d), 0.4 (e), 0.5 (f); y = 0.06 (g), 0.15 (h).

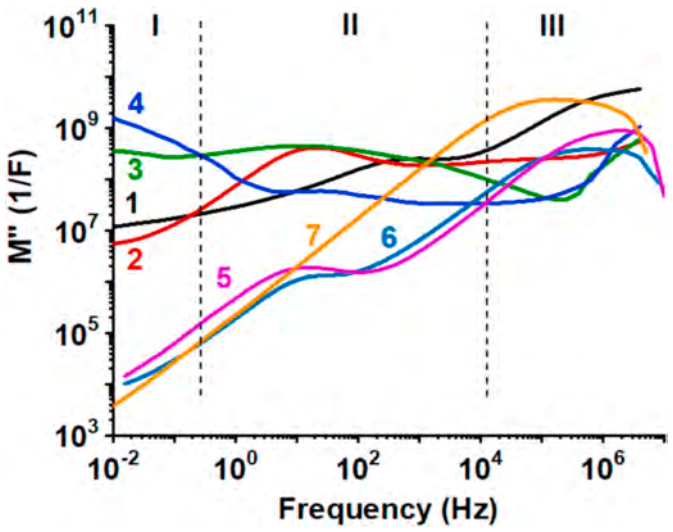

Fig. 3. Frequency dependences of imaginary part of electric modulus of $La_{0.5}Li_{0.5-x}Na_xTiO_3$ and $La_{0.67}Li_{0.2-y}Na_yTi_{0.8}Al_{0.2}O_3$ at $x = 0$ (1), 0.2 (2), 0.3 (3), 0.5 (4); $y = 0$ (5), 0.04 (6), 0.2 (7). Three observed dispersion regions are separated by vertical dotted lines and marked as I-region, II-region and III-region.

$La_{0.67}Na_{0.2}Ti_{0.8}Al_{0.2}O_3$

The final reaction of the $La_{0.67}Li_{0.2-y}Na_yTi_{0.8}Al_{0.2}O_3$ solid solution formation is the interaction of perovskite phases at temperatures above 1200 °C:

$$yLa_{0.67}Li_{0.2}Ti_{0.8}Al_{0.2}O_3 + (1-y)La_{0.67}Na_{0.2}Ti_{0.8}Al_{0.2}O_3 \xrightarrow{1200^\circ C} La_{0.5}Li_{0.5-x}Na_xTiO_3$$

Fig. 2 shows SEM photographs of $La_{0.5}Li_{0.5-x}Na_xTiO_3$ and $La_{0.67}Li_{0.2-y}Na_yTi_{0.8}Al_{0.2}O_3$ samples. The grain size of ceramics in $La_{0.5}Li_{0.5-x}Na_xTiO_3$ and $La_{0.67}Li_{0.2-y}Na_yTi_{0.8}Al_{0.2}O_3$ solid solutions decreases from 5.2 to 2.4 μm (for $x = 0$ and 0.5) and from 6.1 to 1.8 μm (for $y = 0$ and 0.2), respectively. With an increase in sodium concentration, the sintering temperature of solid solutions increases. The driving force for grain growth is related to the reduction of surface and interfacial energy. The limited stage of the grain growth in ceramics is related to the interfacial reactions at interfaces. A decrease in grain size with an increase in sodium concentration can be associated with partial segregation of sodium ions near grain boundaries and a decrease in their mobility [42–45]. In this case, the rate of mass transfer decreases, which leads to the formation of fine-grained ceramics [46–48].

On the spectra of the imaginary part of the complex electrical modulus (Fig. 3) for $La_{0.5}Li_{0.5-x}Na_xTiO_3$ and $La_{0.67}Li_{0.2-y}Na_yTi_{0.8}Al_{0.2}O_3$ solid solutions, three dispersion regions can be distinguished [40]. Low-frequency region I is associated with polarization at the sample-electrode interface. Region II characterizes processes at grain boundaries and high-frequency region III is associated with charge carriers relaxation in grains. As can be seen from Fig. 3 the main contribution to the electrical properties of $La_{0.5}Li_{0.5-x}Na_xTiO_3$ ($0 \le x \le 0.4$) and $La_{0.67}Li_{0.2-y}Na_yTi_{0.8}Al_{0.2}O_3$ ($0 \le x \le 0.15$) solid solutions in a wide frequency range at room temperature is made by dominant process in regions I, II, III. While at high sodium concentrations in $La_{0.5}Li_{0.5-x}Na_xTiO_3$ ($0.45 \le x \le 0.5$) and $La_{0.67}Li_{0.2-y}Na_yTi_{0.8}Al_{0.2}O_3$ ($0.16 \le x \le 0.2$) the main contribution to the electrical properties of solid solutions is made by the dominant ones in regions I and III. This can be attributed to the fact that when lithium is replaced by sodium, the mobility of lithium ions in $La_{0.5}Li_{0.5-x}Na_xTiO_3$ ($0 \le x \le 0.4$) and $La_{0.67}Li_{0.2-y}Na_yTi_{0.8}Al_{0.2}O_3$ ($0 \le x \le 0.15$) decreases as Na^+-ions block the conductivity channels. In this case, lithium remains mobile within the grain. At high sodium concentrations $La_{0.5}Li_{0.5-x}Na_xTiO_3$ ($0.45 \le x \le 0.5$) and $La_{0.67}Li_{0.2-y}Na_yTi_{0.8}Al_{0.2}O_3$ ($0.16 \le x \le 0.2$), the ionic lithium conductivity is absent and the difference between electrical properties in the grain and the grain boundaries disappears, and the material becomes a dielectric.

Fig. 4a shows the complex impedance diagram at room temperature for $La_{0.5}Li_{0.4}Na_{0.1}TiO_3$ and $La_{0.67}Li_{0.16}Na_{0.04}Ti_{0.8}Al_{0.2}O_3$ samples. In the $La_{0.5}Li_{0.4}Na_{0.1}TiO_3$ solid solution, one semicircle, depressed below the real axis, a part of the second semicircle, and a spike at the lowest frequencies are observed. While in $La_{0.67}Li_{0.16}Na_{0.04}Ti_{0.8}Al_{0.2}O_3$ solid solution, the complex impedance spectra show two semicircles and a spike at the lowest frequencies. The arcs at the highest frequencies are shown in the inset to Fig. 4a. For all samples of $La_{0.5}Li_{0.5-x}Na_xTiO_3$ ($0 \le x \le 0.5$) and $La_{0.67}Li_{0.2-y}Na_yTi_{0.8}Al_{0.2}O_3$ ($0 \le y \le 0.2$) solid solutions the real part of the impedance at high frequencies increases with increasing sodium concentration (Fig. 4b).

It has been found that the electrical properties of solid solutions can be analyzed according to the equivalent scheme presented for lanthanum-lithium titanate [40]. It has been illustrated that the main contribution to the electrical properties of ceramic samples is made by three electrically inhomogeneous regions: ceramic's grain (high--frequency region). grain boundary (intermediate frequencies region) and the sample-electrode contact area (low-frequency region).

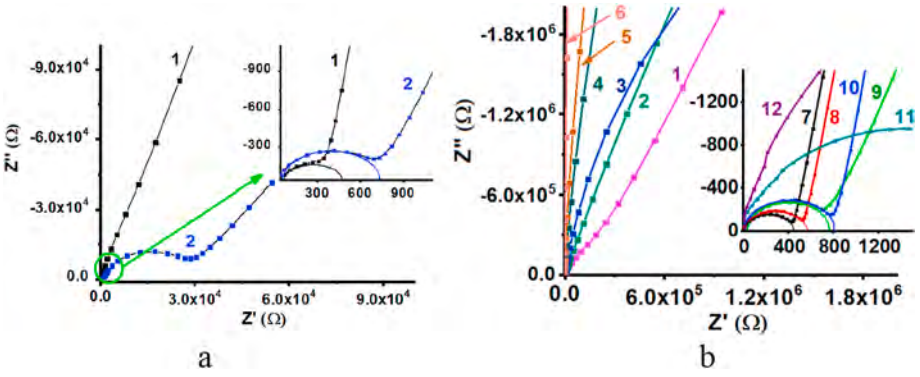

Fig. 4. (a) Complex impedance diagram for $La_{0.5}Li_{0.4}Na_{0.1}TiO_3$ (1) and $La_{0.67}Li_{0.16}Na_{0.04}Ti_{0.8}Al_{0.2}O_3$ (2) ceramic samples. (b) Complex impedance diagram for $La_{0.5}Li_{0.5-x}Na_xTiO_3$ at $x = 0$ (1), 0.1 (2), 0.2 (3), 0.3 (4), 0.4 (5), 0.5 (6) and $La_{0.67}Li_{0.2-y}Na_yTi_{0.8}Al_{0.2}O_3$ at $y = 0$ (7), 0.04 (8), 0.06 (9), 0.1 (10), 0.15 (11), 0.2 (12).

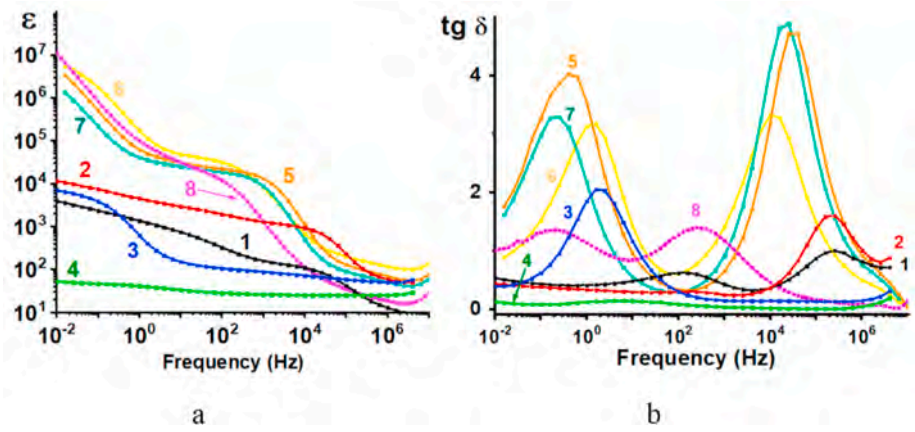

Fig. 5. Dielectric constant (a) and dielectric loss tangent (b) of $La_{0.5}Li_{0.5-x}Na_xTiO_3$ at $x = 0$ (1), 0.1 (2), 0.2 (3), 0.4 (4) and $La_{0.67}Li_{0.2-y}Na_yTi_{0.8}Al_{0.2}O_3$ at $y = 0$ (5), 0.04 (6), 0.1 (7), 0.15 (8).

Table 2
Dielectric constant and dielectric loss tangent in $La_{0.5}Li_{0.5-x}Na_xTiO_3$ and $La_{0.67}Li_{0.2-y}Na_yTi_{0.8}Al_{0.2}O_3$.

$La_{0.5}Li_{0.5-x}Na_xTiO_3$ system						
X	ε′, 1 Hz	ε′, 10 Hz	ε′, 10^2 Hz	ε′, 10^3 Hz	ε′, 10^4 Hz	tan δ (min)
0	1370	743	327	159	109	0.36
0.1	4500	2920	1941	1290	932	0.25
0.2	629	151	106	87.8	87.8	0.29
0.3	61.9	46.2	37.0	32.7	30.6	0.012
0.4	41.3	33.5	28.4	26.3	25.4	0.006
0.5	18.0	17.8	17.6	17.5	17.3	0.003
$La_{0.67}Li_{0.2-y}Na_yTi_{0.8}Al_{0.2}O_3$ system						
Y	ε′, 1 Hz	ε′, 10 Hz	ε′, 10^2 Hz	ε′, 10^3 Hz	ε′, 10^4 Hz	tan δ (min)
0	62347	30634	21912	13260	1113	0.25
0.04	171346	48848	31703	8203	678	0.33
0.06	51521	25315	18107	10957	919	0.31
0.1	40734	24968	18752	8785	499	0.29
0.15	101242	31519	11876	1316	115	0.74
0.2	64896	22210	3618	275	63	0.89

An increase in sodium concentration leads to an increase in ceramic's grain resistance Rg and grain boundaries resistance Rgb for $La_{0.5}Li_{0.5-x}Na_xTiO_3$ ($29.8 \leq Rg \leq 45.2$ Ohm for $0 \leq x \leq 0.4$, $1.74 \cdot 10^3 \leq Rgb \leq 4.64 \cdot 10^7$ Ohm for $0 \leq x \leq 0.5$, for $x = 0.5$ the value of Rg was not observed) and $La_{0.67}Li_{0.2-y}Na_yTi_{0.8}Al_{0.2}O_3$ ($64 \leq Rg \leq 114$ Ohm for $0 \leq y \leq 0.15$, $3.17 \cdot 10^3 \leq Rgb \leq 1.25 \cdot 10^8$ Ohm for $0 \leq y \leq 0.15$ for $x = 0.2$ Rg value was not observed). The electrical properties in the bulk of grains depend on the charge carriers Li^+ concentration and the number of vacancies in the lanthanum sublattice. With an increase in the substitution degree of lithium by sodium, the concentration of charge carriers Li^+ decreases, and the resistance in the grain Rg increases. In addition, the grain size of the ceramics decreases with an increase in sodium concentration, and the total resistance at the grain boundaries Rgb increases.

The frequency dependences of the dielectric constant and dielectric losses for $La_{0.5}Li_{0.5-x}Na_xTiO_3$ and $La_{0.67}Li_{0.2-y}Na_yTi_{0.8}Al_{0.2}O_3$ solid solutions are shown in Fig. 5. It was shown that the samples $La_{0.5}Li_{0.5-x}Na_xTiO_3$ ($0 \leq x \leq 0.1$) and $La_{0.67}Li_{0.2-y}Na_yTi_{0.8}Al_{0.2}O_3$ ($0 \leq y \leq 0.15$) have high values of dielectric permittivity $\varepsilon' > 10^3$ in a wide frequency range (Table 2). There are two relaxation peaks on the curve of dielectric loss tangent are observed, which can be attributed to the coexistence of rhombohedral R-3c and tetragonal phases P4/mmm (Fig. 5b). The maximum permittivity values ϵ_{max} are observed in $La_{0.5}Li_{0.5-x}Na_xTiO_3$ ($x = 0.1$) and $La_{0.67}Li_{0.2-y}Na_yTi_{0.8}Al_{0.2}O_3$ ($y = 0.04$) samples. This can be explained by the fact that with the introduction of a small amount of Na, the unit cell volume increases (Table 1). In this case, the size of the bottleneck and, as a result, the mobility of lithium ions increases, which leads to an increase in the dielectric constant. Further sodium introduction into the $La_{0.5}Li_{0.5-x}Na_xTiO_3$ ($0.2 \leq x \leq 0.5$) and $La_{0.67}Li_{0.2-y}Na_yTi_{0.8}Al_{0.2}O_3$ ($0.06 \leq y \leq 0.2$) solid solutions leads to decrease in dielectric constant. Lithium ions located on the faces of the A-sublattice of perovskite are replaced by sodium ions located in the centers of the A-sublattice [49]. In this case, sodium ions block the movement of lithium ions, reduce the number of vacancies, and charge carriers Li^+. This leads to a decrease in the lithium-ion mobility and a decrease in the dielectric constant.

4. Conclusions

The dielectric properties of $La_{0.5}Li_{0.5-x}Na_xTiO_3$ and $La_{0.67}Li_{0.2-y}Na_yTi_{0.8}Al_{0.2}O_3$ solid solutions obtained by solid-state reaction technique were investigated by the complex impedance spectroscopy. Using full-profile Rietveld analysis it has been shown that the unit cell volume increases with an increase in x and y values. It has been found that the growth of sodium substitution degree leads to a decrease in the ceramic grain size and an increase in resistance at the grain boundary. The dielectric loss increases with increasing in sodium concentration that can be attributed to the fact that substitution of Li by Na decreases the lithium motion and reduces ion conductivity. It has been illustrated that $La_{0.5}Li_{0.4}Na_{0.1}TiO_3$ and $La_{0.67}Li_{0.16}Na_{0.04}Ti_{0.8}Al_{0.2}O_3$ samples had the maximum values of the dielectric constant that can be attributed to a large number of charge carriers Li^+ and the optimal bottleneck size in these materials.

Author statement

Plutenko T.O. – Conceptualization, Investigation, Writing – original draft. V'yunov O.I. – Methodology, Resources, Visualization, Writing – original draft. Yanchevskii O.Z. – Validation, Writing – review & editing. Fedorchuk O.P. – Software, Formal analysis, Investigation. Belous A.G. – Resources, Supervision, Funding acquisition. Plutenko M.O. – Formal analysis, Data curation

Declaration of competing interest

The authors declare that they have no known competing financial interests or personal relationships that could have appeared to influence the work reported in this paper.

Acknowledgements

The work was supported by the Research program of the Ukrainian National Academy of Sciences "New functional substances and materials

for chemical production". The authors acknowledge the CERIC-ERIC Consortium for access to experimental facilities and financial support.

References

[1] J.L. Ndeugueu, M. Aniya, J. Phys. Soc. Jpn. 79 (2010) 72–75, https://doi.org/10.1143/JPSJS.79SA.72.

[2] C.H. Chen, S. Xie, E. Sperling, A.S. Yang, G. Henriksen, K. Amine, Solid State Ionics 167 (2004) 263–272, https://doi.org/10.1016/j.ssi.2004.01.008.

[3] X. Gao, C.A.J. Fisher, Y.H. Ikuhara, Y. Fujiwara, S. Kobayashi, H. Moriwake, A. Kuwabara, K. Hoshikawa, K. Kohama, H. Iba, J. Mater. Chem. 3 (2015) 3351–3359, https://doi.org/10.1039/C4TA07040B.

[4] W.J. Kwon, H. Kim, K.-N. Jung, W. Cho, S.H. Kim, J.-W. Lee, M.-S. Park, J. Mater. Chem. 5 (2017) 6257–6262, https://doi.org/10.1039/C7TA00196G.

[5] Q.N. Pham, M.-P. Crosnier-Lopez, F. Le Berre, F. Fauth, J.-L. Fourquet, Solid State Sci. 6 (2004) 923–929, https://doi.org/10.1016/j.solidstatesciences.2004.05.006.

[6] J.-F. Wu, X. Guo, Phys. Chem. Chem. Phys. 19 (2017) 5880–5887, https://doi.org/10.1039/C6CP07757A.

[7] A.G. Belous, V.I. Butko, G.N. Novitskaia, Y.M. Poplavko, E.F. Ushatkin, Solid State Phys. 27 (1985) 2013–2017.

[8] A.G. Belous, V.I. Butko, G.N. Novitskaya, S.V. Polyanetskaya, Y.M. Poplavko, B. S. Khomenko, Ukrainian J. Phys. 31 (1986) 576–581.

[9] S. Lorant, C. Bohnke, M. Roffat, O. Bohnke, Electrochim. Acta 80 (2012) 418–425, https://doi.org/10.1016/j.electacta.2012.07.051.

[10] A. Belous, G. Kolbasov, L. Kovalenko, E. Boldyrev, S. Kobylianska, B. Liniova, J. Solid State Electrochem. 22 (2018) 2315–2320, https://doi.org/10.1007/s10008-018-3943-x.

[11] Y. Inaguma, C. Liquan, M. Itoh, T. Nakamura, T. Uchida, H. Ikuta, M. Wakihara, Solid State Commun. 86 (1993) 689–693, https://doi.org/10.1016/0038-1098(93)90841-A.

[12] Y. Inaguma, M. Itoh, Solid State Ionics 86 (1996) 257–260, https://doi.org/10.1016/0167-2738(96)00100-2.

[13] A.G. Belous, O.V. Ovchar, J. Eur. Ceram. Soc. 23 (2003) 2525–2528, https://doi.org/10.1016/S0955-2219(03)00185-7.

[14] A.G. Belous, S.D. Kobylianska, Lithium Conducting Solid Oxide Electrolytes, Naukova Dumka, Kyiv, 2018. http://library.kpi.kharkov.ua/ru/chemistry_Okclte.

[15] A.G. Belous, J. Eur. Ceram. Soc. 21 (2001) 1797–1800, https://doi.org/10.1016/S0955-2219(01)00118-2.

[16] H.-T. Chung, J.-G. Kim, H.-G. Kim, Solid State Ionics 107 (1998) 153–160, https://doi.org/10.1016/S0167-2738(97)00525-0.

[17] O. Bohnke, C. Bohnke, J. Ould Sid'Ahmed, M.P. Crosnier-Lopez, H. Duroy, F. Le Berre, J.L. Fourquet, Chem. Mater. 13 (2001) 1593–1599, https://doi.org/10.1021/cm001207u.

[18] A. Rivera, C. León, J. Santamaría, A. Várez, O. V'yunov, A.G. Belous, J.A. Alonso, J. Sanz, Chem. Mater. 14 (2002) 5148–5152, https://doi.org/10.1021/cm0204627.

[19] J.A. Alonso, J. Sanz, J. Santamaría, C. León, A. Várez, M.T. Fernández- Díaz, Angew. Chem. 112 (2000) 633–635, https://doi.org/10.1002/(SICI)1521-3757(20000204)112:3<633::AID-ANGE633>3.0.CO;2-R.

[20] X. Zhang, W. Chen, J. Wang, Y. Shen, L. Gu, Y. Lin, C.-W. Nan, Nanoscale 6 (2014) 6701–6709, https://doi.org/10.1039/C4NR00703D.

[21] W. Jia, Y. Hou, M. Zheng, M. Zhu, J. Alloys Compd. 724 (2017) 306–315, https://doi.org/10.1016/j.jallcom.2017.07.030.

[22] Y. Qu, D. Shan, J. Song, Mater. Sci. Eng., B 121 (2005) 148–151, https://doi.org/10.1016/j.mseb.2005.03.023.

[23] F. Han, J. Deng, X. Liu, T. Yan, S. Ren, X. Ma, S. Liu, B. Peng, L. Liu, Ceram. Int. 43 (2017) 5564–5573, https://doi.org/10.1016/j.ceramint.2017.01.086.

[24] I.P. Raevski, S.A. Prosandeev, A.S. Bogatin, M.A. Malitskaya, L. Jastrabik, J. Appl. Phys. 93 (2003) 4130–4136, https://doi.org/10.1063/1.1558205.

[25] Z.-M. Dang, B. Peng, D. Xie, S.-H. Yao, M.-J. Jiang, J. Bai, Appl. Phys. Lett. 92 (2008) 112910, https://doi.org/10.1063/1.2894571.

[26] G. Subodh, V. Deepu, P. Mohanan, M.T. Sebastian, Appl. Phys. Lett. 95 (2009), 062903, https://doi.org/10.1063/1.3200244.

[27] Z.M. Dang, T. Zhou, S.H. Yao, J.K. Yuan, J.W. Zha, H.T. Song, J.Y. Li, Q. Chen, W. T. Yang, J. Bai, Adv. Mater. 21 (2009) 2077–2082, https://doi.org/10.1002/adma.200803427.

[28] A. Ameli, M. Nofar, C.B. Park, P. Pötschke, G. Rizvi, Carbon 71 (2014) 206–217, https://doi.org/10.1016/j.carbon.2014.01.031.

[29] F. He, S. Lau, H.L. Chan, J. Fan, Adv. Mater. 21 (2009) 710–715, https://doi.org/10.1002/adma.200801758.

[30] G.P. Mazzara, S. Skirius, G. Cao, G. Chern, R. Clark, J.E. Crow, H. Mathias, J. W. O'Reilly, L.R. Testardi, Phys. Rev. B 47 (1993) 8119, https://doi.org/10.1103/PhysRevB.47.8119.

[31] F.B. Madsen, L. Yu, A.E. Daugaard, S. Hvilsted, A.L. Skov, Polymer 55 (2014) 6212–6219, https://doi.org/10.1016/j.polymer.2014.09.056.

[32] J. Wu, C.-W. Nan, Y. Lin, Y. Deng, Phys. Rev. Lett. 89 (2002) 217601, https://doi.org/10.1103/PhysRevLett.89.217601.

[33] Y. Yang, B.-P. Zhu, Z.-H. Lu, Z.-Y. Wang, C.-L. Fei, D. Yin, R. Xiong, J. Shi, Q.-G. Chi, Q.-Q. Lei, Appl. Phys. Lett. 102 (2013), 042904, https://doi.org/10.1063/1.4789504.

[34] P. Thongbai, T. Yamwong, S. Maensiri, Solid State Commun. 147 (2008) 385–387, https://doi.org/10.1016/j.ssc.2008.06.020.

[35] C.-L. Huang, K.-H. Chiang, Mater. Res. Bull. 39 (2004) 1701–1708, https://doi.org/10.1016/j.materresbull.2004.05.003.

[36] W. Wu, X. Huang, S. Li, P. Jiang, J. Phys. Chem. C 116 (2012) 24887–24895, https://doi.org/10.1021/jp3088644.

[37] G. Ioannou, A. Patsidis, G.C. Psarras, Compos. Appl. Sci. Manuf. 42 (2011) 104–110, https://doi.org/10.1016/j.compositesa.2010.10.010.

[38] S. García-Martín, A. Morata-Orrantia, M.H. Aguirre, M.Á. Alario-Franco, Appl. Phys. Lett. 86 (2005), 043110, https://doi.org/10.1063/1.1852717.

[39] T.O. Plutenko, O.I. V'yunov, B.S. Khomenko, A.G. Belous, UCJ 86 (2020) 13–23, https://doi.org/10.33609/2708-129X.86.11.2020.13-23.

[40] E. Kazakevičius, A. Kežionis, T. Šalkus, A.F. Orliukas, O.I. V'yunov, L.L. Kovalenko, A.G. Belous, Funct. Mater. Lett. 8 (2015), https://doi.org/10.1142/S1793604715500769, 1550076-1550071 – 1550076-1550075.

[41] M.L. Sanjuan, M.A. Laguna, A.G. Belous, O.I. V'yunov, Chem. Mater. 17 (2005) 5862–5866, https://doi.org/10.1021/cm0517770.

[42] S.B. Desu, D.A. Payne, J. Am. Ceram. Soc. 73 (1990) 3398–3406, https://doi.org/10.1111/j.1151-2916.1990.tb06467.x.

[43] M. Shirpour, B. Rahmati, W. Sigle, P.A. van Aken, R. Merkle, J. Maier, J. Phys. Chem. C 116 (2012) 2453–2461, https://doi.org/10.1021/jp208213x.

[44] D.J. Kubicki, D. Prochowicz, A. Hofstetter, S.M. Zakeeruddin, M. Grätzel, L. Emsley, J. Am. Chem. Soc. 140 (2018) 7232–7238, https://doi.org/10.1021/jacs.8b03191.

[45] C. Zhou, X. Liu, W. Li, C. Yuan, Mater. Chem. Phys. 114 (2009) 832–836, https://doi.org/10.1016/j.matchemphys.2008.10.063.

[46] A.G. Belous, Ionics 4 (1998) 360–363, https://doi.org/10.1007/BF02375878.

[47] D.R. Lide, Handbook of Chemistry and Physics, 86th ed., CRC Press, Taylor & Francis, Boca Raton, FL, 2005 https://doi.org/10.1021/ja059868l.

[48] A.E. Newkirk, I. Aliferis, Anal. Chem. 30 (1958) 982–984, https://doi.org/10.1021/ac60137a031.

[49] C.P. Herrero, A. Varez, A. Rivera, J. Santamaría, C. León, O.I. V'yunov, A. G. Belous, J. Sanz, J. Phys. Chem. B 109 (2005) 3262–3268, https://doi.org/10.1021/jp046076p.